Hyperuniformity, quasi-long-range correlations, and void-space constraints in maximally random jammed particle packings. I. Polydisperse spheres

Chase E. Zachary*

Department of Chemistry, Princeton University, Princeton, New Jersey 08544, USA

Yang Jiao†

Department of Mechanical and Aerospace Engineering, Princeton University, Princeton, New Jersey 08544, USA

Salvatore Torquato‡

Department of Chemistry, Department of Physics, Princeton Center for Theoretical Science, Program in Applied and Computational Mathematics, and Princeton Institute for the Science and Technology of Materials, Princeton University, Princeton, New Jersey 08544, USA

Abstract

Hyperuniform many-particle distributions possess a local number variance that grows more slowly than the volume of an observation window, implying that the local density is effectively homogeneous beyond a few characteristic length scales. Previous work on maximally random strictly jammed sphere packings in three dimensions has shown that these systems are hyperuniform and possess unusual quasi-long-range pair correlations decaying as r^{-4}, resulting in anomalous logarithmic growth in the number variance. However, recent work on maximally random jammed sphere packings with a size distribution has suggested that such quasi-long-range correlations and hyperuniformity are not universal among jammed hard-particle systems. In this paper we show that such systems are indeed hyperuniform with signature quasi-long-range correlations by characterizing the more general local-volume-fraction fluctuations. We argue that the regularity of the void space induced by the constraints of saturation and strict jamming overcomes the local inhomogeneity of the disk centers to induce hyperuniformity in the medium with a linear small-wavenumber nonanalytic behavior in the spectral density, resulting in quasi-long-range spatial correlations scaling with $r^{-(d+1)}$ in d Euclidean space dimensions. A numerical and analytical analysis of the pore-size distribution for a binary MRJ system in addition to a local characterization of the n-particle loops governing the void space surrounding the inclusions is presented in support of our argument. This paper is the first part of a series of two papers considering the relationships among hyperuniformity, jamming, and regularity of the void space in hard-particle packings.

* czachary@princeton.edu

† yjiao@princeton.edu

‡ torquato@princeton.edu

I. INTRODUCTION

Maximally random jammed (MRJ) packings of hard particles are the most disordered structures, according to some well-defined order metrics, that are rigorously incompressible and nonshearable [1]. These systems are prototypical "glassy" structures in the sense that they are structurally rigid yet lack Bragg peaks in their scattering spectra [2]. In this sense, the idea of the MRJ state has replaced the mathematically ill-defined notion of random close packing [1]. Nearly half-a-century ago these systems were thought to describe the disordered structure of liquids [3], but it is now known that three-dimensional MRJ monodisperse sphere packings possess unusual quasi-long-range (QLR) pair correlations decaying as r^{-4} [4]. This property is markedly different from typical liquids, in which pair correlations decay exponentially fast [2, 5, 6]. Similar QLR behavior has also been observed in noninteracting spin-polarized fermionic ground states [7, 8], the ground state of liquid helium [9], and the Harrison-Zeldovich power spectrum of the density fluctuations of the early Universe [10]. However, for each of these examples and for MRJ hard sphere packings, the structural origins of these correlations have been heretofore unknown, even for monodisperse systems. Furthermore, it is an open problem to generalize these QLR correlations for MRJ states to polydisperse packings, in which the jamming properties are intimately related to the size-distribution of the particles [11].

Motivated by the observation that MRJ packings are structurally rigid with a well-defined contact network, Torquato and Stillinger conjectured [5] that all strictly jammed (i.e., mechanically rigid), saturated [12] packings of monodisperse spheres in d-dimensional Euclidean space $\mathbb{R}^d$ are hyperuniform, meaning that infinite-wavelength local density fluctuations vanish [5], a proposition for which no counterexample has been found to date [13]. This conjecture suggests that saturation and strict jamming are sufficient to induce hyperuniformity, albeit not necessary [5]. Hyperuniform systems play an integral role in understanding the relationship between fluctuations in local material properties and microstructural order [4–6, 14–16]. These systems have applications to the large-scale structure of the Universe [10], the structure and collective motion of grains in vibrated granular media [17], the structure of living cells [18], transport through composites and porous media [19], the study of noise and granularity of photographic images [20, 21], identifying properties of organic coatings [22], and the fracture of composite materials [23]. For microstructures consisting of "point"

particles, one considers fluctuations in the local number density within some observation window. Hyperuniform point patterns possess local density fluctuations that asymptotically grow more slowly than the volume of the window. Recently, the concept of hyperuniformity has been extended to include systems composed of finite-volume inclusions of arbitrary geometries [6]; in these cases, the quantity of interest is the fluctuation in the so-called local volume fraction, defined as the fraction of the volume within an observation window covered by a given phase. Hyperuniform heterogeneous media possess local-volume-fraction fluctuations that asymptotically decay faster than the volume of the observation window, implying that the local volume fraction approaches a global value beyond relatively few characteristic length scales.

Previous work on three-dimensional (3D) MRJ monodispere sphere packings [4] has supported the Torquato-Stillinger conjecture by showing that the structure factor $S(k)$, proportional to the scattering intensity, approaches zero linearly as the wavenumber $k \to 0$, inducing a QLR power-law tail r^{-4} in the pair correlation function $g_2(r)$. This behavior implies that local-number-density fluctuations grow logarithmically faster than the surface area of an observation window but still slower than the window volume. In this sense, the "degree" of hyperuniformity in MRJ packings is minimal among all strictly jammed saturated packings. However, recent numerical [24] and experimental [25] work on polydisperse MRJ packings has suggested that hyperuniform quasi-long-range correlations are not a universal signature of the MRJ state. Unlike monodisperse systems, the distribution of particle sizes in a polydisperse packing introduces locally inhomogeneous regions as the particles distribute themselves through space as shown in Figure 1. One can see in the binary packing that local clusters of small particles are distributed near and around larger inclusions, and the result is that the point pattern generated by the disk centers possesses local inhomogeneities that are expected to (and indeed do) induce volume-order scaling within the number variance. The situation is apparently even more complex for the polydisperse system in Figure 1 since the size distribution results in a highly inhomogeneous local structure with small particles trapped between larger ones with a high probability.

These observations have raised a number of quantitatively and conceptually difficult questions. First, what is the appropriate extension of the Torquato-Stillinger conjecture for monodisperse MRJ packings to systems with a size distribution? Clearly, one must explicitly account for the shape information of the particles. Second, in the event that one

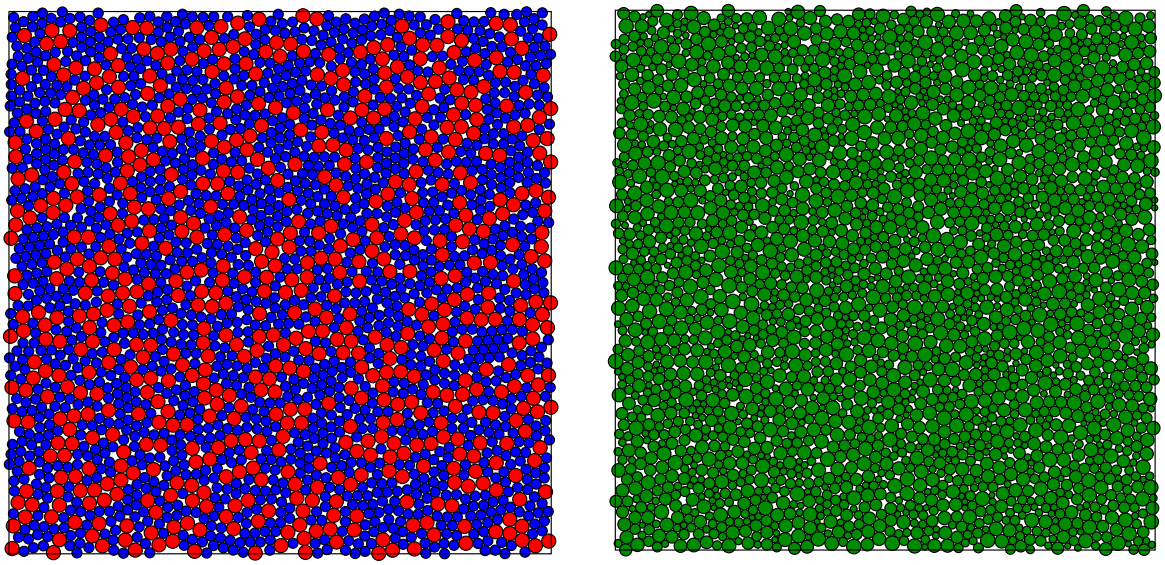

(a) **(b)**

FIG. 1. (Color online) (a) A binary packing of hard disks near the MRJ state. (b) A polydisperse packing of hard disks near the MRJ state.

can generalize the Torquato-Stillinger conjecture, there is to date no satisfactory structural explanation for the *linear* small-wavenumber scaling of the structure factor observed for 3D MRJ monodisperse hard sphere packings, which indicates the presence of QLR pair correlations. This extraordinarily difficult problem is tantamount to providing an analytical prediction of the MRJ state. Unfortunately, no such rigorous theory currently exists, even for the considerably simpler problem of predicting the scalar MRJ density [26]. The presence of QLR correlations makes this problem inherently nonlocal, and, therefore, methods that attempt to predict the MRJ state based only on packing fraction and local criteria, such as nearest-neighbor and Voronoi statistics, are invariably incomplete [26].

We have presented arguments in a recent letter to suggest strongly that hyperuniformity and quasi-long-range pair correlations are signatures of saturated MRJ packings of hard particles, including binary disks, ellipses, and superdisks [27]. In this paper, we provide detailed evidence to show that polydisperse MRJ packings of hard spheres, though inhomogeneous with respect to the number variance, possess local-volume-fraction fluctuations decaying faster than the volume of an observation window. This observation is consistent with the generalized Torquato-Stillinger conjecture that all strictly jammed saturated pack-

ings of spheres are hyperuniform with respect to fluctuations in the *local volume fraction*. Our major results include:

1. Infinite wavelength local number density fluctuations do not vanish for MRJ packings of polydisperse hard spheres. Local-volume-fraction fluctuations provide the appropriate structural description of these packings because they account correctly for the size distribution of the particles. Importantly, our work studying local-volume-fraction fluctuations contains previously-published results for 3D monodisperse MRJ hard sphere packings as a special case.

2. Signature QLR pair correlations scaling asymptotically as $r^{-(d+1)}$ in d Euclidean dimensions are observed for all systems that we study, including binary disks with varying size ratios and compositions and polydisperse disk packings. Our results suggest that these special correlations may be a universal feature of the MRJ state.

3. Strict jamming places a strong constraint on the distribution of the available void space external to the particles such that hyperuniformity is observed when considering local-volume-fraction fluctuations, even when the point pattern of the sphere centers is locally inhomogeneous.

4. The competition between maximal randomness and strict jamming of the packings ensures that the void-space distribution is sufficiently broad to induce QLR correlations between particles, thereby providing a direct qualitative *structural* explanation for the linear small-wavenumber region of the generalized scattering intensity.

II. BACKGROUND AND DEFINITIONS

A. Point patterns

We consider point patterns to be realizations of stochastic point processes. Formally, a *stochastic point process* is a method of placing points in some space (such as $\mathbb{R}^d$) according to an underlying probability distribution. This random setting is quite general, incorporating cases in which the locations of the points are deterministically known, such as in a Bravais lattice [28].

A statistically homogeneous point process is completely determined by the number density ρ and the countably infinite set (in the thermodynamic limit) of *n-particle correlation functions*. The n-particle correlation function $g_n(\mathbf{r}_1, \ldots, \mathbf{r}_n)$ is proportional to the probability density of finding n particles in volume elements around the positions $\mathbf{r}_1, \ldots, \mathbf{r}_n$, regardless of the positions of the remaining particles in the system. For an arbitrary point process, deviations of g_n from unity provide a measure of the correlations among points in the system. Note that specifying only a finite number M of the n-particle correlation functions defines a class of microstructures with degenerate M-particle statistics [29]. Of particular interest is the pair correlation function g_2, which defines the average number of particles surrounding a reference particle of the point process. Closely related to the pair correlation function is the *total correlation function* $h(\mathbf{r}) = g_2(\mathbf{r}) - 1$. Since $g_2(r) \to 1$ as $r \to +\infty$ ($r = \|\mathbf{r}\|$) for isotropic, translationally invariant systems without long-range order, it follows that $h(r) \to 0$ in this limit, meaning that h is generally integrable with a well-defined Fourier transform.

It is common in statistical mechanics when passing to reciprocal space to consider the associated *structure factor* $S(k)$, which for a translationally invariant system is defined by

$$S(k) = 1 + \rho\hat{h}(k), \tag{1}$$

where $\hat{h}$ is the Fourier transform of the total correlation function, ρ is the number density, and $k = \|\mathbf{k}\|$ is the magnitude of the reciprocal variable to $\mathbf{r}$. We utilize the following definition of the Fourier transform:

$$\hat{f}(\mathbf{k}) = \int_{\mathbb{R}^d} f(\mathbf{r}) \exp\left(-i\mathbf{k}\cdot\mathbf{r}\right) d\mathbf{r}, \tag{2}$$

where $\mathbf{k}\cdot\mathbf{r} = \sum_{i=1}^{d} k_i r_i$ is the conventional Euclidean inner product of two real-valued vectors. For radially-symmetric functions [i.e., $f(\mathbf{r}) = f(\|\mathbf{r}\|) = f(r)$], the Fourier transform may be written

$$\hat{f}(k) = (2\pi)^{d/2} \int_0^\infty r^{d-1} f(r) \frac{J_{(d/2)-1}(kr)}{(kr)^{(d/2)-1}} dr. \tag{3}$$

B. Two-phase random heterogeneous media

Closely related to the notion of a stochastic point process is that of a two-phase random heterogeneous medium (or random set), which we define to be a domain of space $\mathcal{V} \subseteq \mathbb{R}^d$ of

volume $V \leq +\infty$ that is composed of two regions: the phase 1 region $\mathcal{V}_1$ of volume fraction ϕ_1 and the phase 2 region $\mathcal{V}_2$ of volume fraction ϕ_2 [30]. The statistical properties of each phase of the system are specified by the countably infinite set of *n-point probability functions* $S_n^{(i)}$, which are defined by [11, 31–33]

$$S_n^{(i)}(\mathbf{r}_1, \ldots, \mathbf{r}_n) = \left\langle \prod_{i=1}^{n} I^{(i)}(\mathbf{r}_i) \right\rangle, \tag{4}$$

where $I^{(i)}$ is the indicator function for phase i

$$I^{(i)}(\mathbf{x}) = \begin{cases} 1, & \mathbf{x} \in \mathcal{V}_i \\ 0, & \text{else.} \end{cases} \tag{5}$$

The function S_n defines the probability of finding n points at positions $\mathbf{r}_1, \ldots, \mathbf{r}_n$ all within the same phase.

Upon subtracting the long-range behavior from S_2, one obtains the autocovariance function $\chi(\mathbf{r}) = S_2(\mathbf{r}) - \phi^2$, which is generally integrable. It is important to recognize that the autocovariance function is independent of the choice of reference phase, meaning that it is a *global* descriptor of correlations within the system. This property will play a particularly important role in this paper when we consider the relationship between local-volume-fraction fluctuations and the void space between inclusions in the microstructure. The analog of the structure factor in this context is the so-called *spectral density*, which is the Fourier transform $\hat{\chi}$ of the autocovariance function [34]. The autocovariance function obeys the bounds [11]

$$-\min\{(1-\phi)^2, \phi^2\} \leq \chi(\mathbf{r}) \leq (1-\phi)\phi, \tag{6}$$

where ϕ is the volume fraction of an arbitrary reference phase. We remark that it is an open problem to identify additional necessary and sufficient conditions that the autocovariance function must satisfy in order to correspond to a binary stochastic process [11, 35–38].

C. Sphere packings and a categorization of jamming

A *sphere packing* is a collection of non-overlapping spheres in d-dimensional Euclidean space $\mathbb{R}^d$. The *packing density* ϕ (equivalent to the volume fraction of the particle phase) is defined as the fraction of space covered by the spheres, which may be polydisperse. An

important characteristic of a packing is its degree of randomness (or the antithesis, order), which reflects nontrivial information of the packing structure. The degree of randomness (order) can be quantified by a set of *order metrics* ψ [1]. It is an open and challenging problem to identify good order metrics, but it has recently been proposed that hyperuniformity is itself a measure of order on large length scales [5, 6].

One method of classifying sphere packings involves characterizing the extent to which particles are *jammed*. Torquato and Stillinger [39, 40] have provided a precise definition of the term *jamming* and have proposed a hierarchical classification scheme for sphere packings by invoking the notions of *local*, *collective*, and *strict* jamming. A packing is *locally* jammed if no particle in the system can be translated while fixing the positions of all other particles. A *collectively* jammed packing is locally jammed such that no subset of spheres can simultaneously be continuously displaced without moving its members out of contact both with one another and with the remainder set. A packing is *strictly* jammed if it is collectively jammed and if all globally uniform volume nonincreasing deformations of the system boundary are disallowed by the impenetrability constraints. The reader is referred to Ref. [39] for further details.

As previously mentioned, the *maximally random jammed* (MRJ) state is defined as the most disordered jammed packing in a given jamming category (i.e., locally, collectively, or strictly jammed) [1]. The MRJ state is well-defined for a given jamming category and choice of order metric, and it has recently supplanted the ill-defined random close packed (RCP) state [1]. In this paper, we focus on maximally random strictly jammed polydisperse sphere packings in $\mathbb{R}^d$.

D. Hyperuniformity in point processes: local number density fluctuations

A *hyperuniform point process* has the property that the variance in the number of points in an observation window Ω grows more slowly than the volume of that window. In the case of a spherical observation window, this definition implies that the local number variance $\sigma_N^2(R)$ grows more slowly than R^d in d dimensions, where R is the radius of the observation window. Torquato and Stillinger [5] have provided an exact expression for the local number

variance of a statistically homogeneous point process in a spherical observation window

$$\sigma_N^2(R) = \rho v(R)\left[1 + \rho \int_{\mathbb{R}^d} h(\mathbf{r})\alpha(r;R)d\mathbf{r}\right], \tag{7}$$

where R is the radius of the observation window, $v(R)$ is the volume of the window, and $\alpha(r;R)$ is the so-called *scaled intersection volume*. The latter quantity is geometrically defined as the volume of space occupied by the intersection of two spheres of radius R separated by a distance r and normalized by the volume of a sphere $v(R)$. Exact expressions for $\alpha(r;R)$ in arbitrary dimensions have been given by Torquato and Stillinger [41].

It is convenient to introduce a dimensionless density ϕ, which need not correspond to the volume fraction, according to

$$\phi = \rho v(D/2) = \frac{\rho \pi^{d/2} D^d}{2^d \Gamma(1 + d/2)}, \tag{8}$$

where D is a characteristic length scale of the system (e.g., the mean nearest-neighbor distance between points). The number variance admits the following asymptotic scaling [5]:

$$\sigma_N^2(R) = 2^d \phi \left\{ A_N \left(\frac{R}{D}\right)^d + B_N \left(\frac{R}{D}\right)^{d-1} + o\left[\left(\frac{R}{D}\right)^{d-1}\right]\right\}, \tag{9}$$

where $o(x)$ denotes all terms of order less than x. This result is valid for all periodic point patterns (including lattices), quasicrystals that possess Bragg peaks, and disordered systems in which the pair correlation function g_2 decays to unity exponentially fast [5]. Explicit forms for the asymptotic coefficients A_N and B_N are given by [5]

$$A_N = 1 + \rho \int_{\mathbb{R}^d} h(\mathbf{r})d\mathbf{r} = \lim_{\|\mathbf{k}\|\to 0} S(\mathbf{k}) \tag{10}$$

$$B_N = -\frac{\rho \kappa(d)}{D} \int_{\mathbb{R}^d} h(\mathbf{r})\|\mathbf{r}\| d\mathbf{r}, \tag{11}$$

where $\kappa(d) = \Gamma(1 + d/2)/\{\pi^{1/2}\Gamma[(d+1)/2]\}$.

Any system with $A_N = 0$ satisfies the requirements for hyperuniformity. Although the expansion (9) will hold for all periodic and quasiperiodic point patterns with Bragg peaks, this behavior is not generally true for disordered hyperuniform systems. For example, it is known that if the total correlation function $h \sim r^{-(d+1)}$ for large r [$S(k) \sim k$ for small k], then $\sigma_N^2(R) \sim (a_0 \ln R + a_1)R^{d-1}$ [7]. Such behavior occurs in maximally random jammed monodisperse sphere packings in three dimensions [4] and noninteracting spin-polarized fermion ground states [7, 8]. Other examples of "anomalous" local density fluctuations have been characterized by Zachary and Torquato [6].

E. Hyperuniformity in two-phase random heterogeneous media: local-volume-fraction fluctuations

In order to define hyperuniformity for heterogeneous media we introduce the *local volume fraction* $\tau_i(\mathbf{x})$ of phase i according to

$$\tau_i(\mathbf{x}; R) = \frac{1}{v(R)} \int I^{(i)}(\mathbf{z}) w(\mathbf{z} - \mathbf{x}; R) d\mathbf{z}, \tag{12}$$

where $v(R)$ is the volume of the observation window and w is the corresponding indicator function. Using this definition, the variance $\sigma_\tau^2(R)$ in the local volume fraction is given by

$$\sigma_\tau^2(R) = \frac{1}{v(R)} \int_{\mathbb{R}^d} \chi(\mathbf{r}) \alpha(r; R) d\mathbf{r}, \tag{13}$$

which is independent of the choice of reference phase. The variance in the local volume fraction admits the asymptotic expansion [6]

$$\sigma_\tau^2 = \frac{\rho}{2^d \phi} \left\{ A_\tau \left(\frac{D}{R} \right)^d + B_\tau \left(\frac{D}{R} \right)^{d+1} + o\left[\left(\frac{D}{R} \right)^{d+1} \right] \right\} \tag{14}$$

$$A_\tau = \int_{\mathbb{R}^d} \chi(\mathbf{r}) d\mathbf{r} = \lim_{\|\mathbf{k}\| \to 0} \hat{\chi}(\mathbf{k}) \tag{15}$$

$$B_\tau = -\frac{\kappa(d)}{D} \int_{\mathbb{R}^d} \|\mathbf{r}\| \chi(\mathbf{r}) d\mathbf{r}. \tag{16}$$

The coefficients A_τ and B_τ in (15) and (16) control the asymptotic scaling of the fluctuations in the local volume fraction. It then follows that σ_τ^2 decays faster than R^{-d} as $R \to +\infty$ for those systems such that

$$\lim_{\|\mathbf{k}\| \to 0} \hat{\chi}(\mathbf{k}) = 0, \tag{17}$$

which defines a hyperuniform two-phase random heterogeneous medium [6].

F. The effect of polydispersity on local fluctuations

Here we consider how the presence of polydispersity in a sphere packing affects the fluctuations in the local number density and local volume fraction. For a packing of polydisperse spheres, the distribution of sphere radii is determined by a probability density $f(R)$, and the fundamental statistical descriptors of the medium therefore involve averages $\langle \cdot \rangle_R$ [42] over the distribution of sphere sizes [11]. For a packing of polydisperse spheres with M distinct

radii, the density function $f(R)$ takes the form

$$f(R) = \sum_{i=1}^{M} \gamma_i \delta(R - R_i), \tag{18}$$

where $\gamma_i = N_i/N$ is the mole fraction of species i. As an example, we will continually refer in this paper to the average particle diameter $\langle D \rangle_R$ of a polydisperse hard-disk packing:

$$\langle D \rangle_R = \sum_{i=1}^{M} \gamma_i D_i, \tag{19}$$

where D_i is the diameter of species i.

The autocovariance function $\chi(\mathbf{r})$ for a heterogeneous medium consisting of impenetrable polydisperse spheres is given by [11, 43, 44]

$$\chi(\mathbf{r}) = \rho \langle v_{\text{int}}(\mathbf{r}; R) \rangle_R + \rho^2 \int \langle h(\mathbf{x}; R_1, R_2) v_{\text{int}}(\mathbf{r} - \mathbf{x}; R_1, R_2) \rangle_{R_1,R_2} \, d\mathbf{x}, \tag{20}$$

which implies that

$$A_\tau = \int \chi(\mathbf{r}) d\mathbf{r} \tag{21}$$

$$= \rho \langle v^2(R) \rangle_R + \rho^2 \left\langle v(R_1) v(R_2) \int h(\mathbf{r}; R_1, R_2) d\mathbf{r} \right\rangle_{R_1,R_2}. \tag{22}$$

Unlike for monodisperse sphere packings [6], the result (22) shows that it is generally not possible to separate the shape information of the inclusions from the details of the point pattern generated by the sphere centers. This observation suggests that for polydisperse microstructures, hyperuniformity of the underlying point pattern does not induce hyperuniformity with respect to local-volume-fraction fluctuations; conversely, it is also possible to find heterogeneous media for which $A_\tau = 0$ but $A_N > 0$.

We note that the first term contributing to $\chi(\mathbf{r})$ in (20) can be interpreted as the probability of finding two points, separated by a displacement $\mathbf{r}$, in a single particle of the packing. The second term is therefore related to the probability of finding the points in two different particles. It is clear that only this latter term, containing the pair correlation function, can contribute to the linear small-wavenumber region of the spectral density, and it is therefore responsible, albeit in a highly nontrivial way, for the onset of QLR correlations in MRJ packings.

III. LOCAL DENSITY AND VOLUME FRACTION FLUCTUATIONS IN POLYDISPERSE MRJ PACKINGS

A. Generation of MRJ polydisperse hard disk packings

Motivated by the generalized conjecture that all strictly jammed packings of d-dimensional spheres are hyperuniform with respect to local-volume-fraction fluctuations, we have generated several packings of binary disks (2D) near the MRJ state using a modified Lubachevsky-Stillinger (LS) packing algorithm [45–49], wherein particles with a fixed size ratio undergo event-driven molecular dynamics while simultaneously increasing in size according to some prescribed growth rate. The initial growth rate used in our simulations is $\gamma = 0.01$, but near the jamming point, a much smaller growth rate $\gamma = 10^{-6}$ is used to establish well-defined interparticle contacts. The Lubachevsky-Stillinger algorithm has been shown to produce MRJ packings with these parameters consistent with the positively-correlated translational and orientational order metrics [50, 51]. Our statistics for binary packings are averaged over 50 configurations of 10000 particles; for polydisperse packings we have averaged over 10 configurations of 10000 particles. Our results have been compared to systems of up to 10^6 particles to verify invariance of the statistics with respect to system size.

For this study, we have chosen a particle size ratio $\beta = R_{\text{large}}/R_{\text{small}} = 1.4$ and mole fractions $\gamma_{\text{small}} = 0.75$ and $\gamma_{\text{large}} = 0.25$; however, the focus of this study is to elucidate a universal property of polydisperse MRJ packings, and our results are expected to apply for a range of size ratios, size distributions, and mole fractions (see Figure 2) [52]. For the remainder of this paper, we therefore focus on the binary case with the disclaimer that our results are expected to apply for general polydisperse MRJ packings. This algorithm has been used in previous studies of 3D monodisperse sphere packings near the MRJ state [47]. The resulting packings in this study have a final volume fraction $\phi \approx 0.8475$, which is below the the close-packed density $\phi_{\text{cp}} = \sqrt{3}\pi/6$. Figure 1 (Section I) provides a typical realization of a binary packing; note that the particle distribution is saturated and nonperiodic.

B. Hyperuniformity and local-volume-fraction fluctuations

We have calculated both the structure factor $S(k)$ and the spectral density $\hat{\chi}(k)$ for the binary MRJ disk packings using discrete Fourier transforms of the local density $\rho(\mathbf{r})$ and

indicator function $I(\mathbf{r})$ of the particle phase of the packing. Specifically,

$$S(\mathbf{k}) = \frac{\left|\sum_{j=1}^{N} \exp\left(-i\mathbf{k}\cdot\mathbf{r}_j\right)\right|^2}{N} \qquad (\mathbf{k} \neq \mathbf{0}) \tag{23}$$

$$\hat{\chi}(\mathbf{k}) = \frac{\left|\sum_{j=1}^{N} \exp\left(-i\mathbf{k}\cdot\mathbf{r}_j\right)\hat{m}(\mathbf{k}; R_j)\right|^2}{V} \qquad (\mathbf{k} \neq \mathbf{0}), \tag{24}$$

where

$$\hat{m}(\mathbf{k}; R) \equiv \int_{\mathbb{R}^d} \exp(-i\mathbf{k}\cdot\mathbf{r})\Theta(R - \|\mathbf{r}\|)d\mathbf{r} \tag{25}$$

is the Fourier transform of the indicator function for a d-dimensional sphere of radius R [53]. Note that the shape of the enclosure (defined by a set of basis vectors $\{\mathbf{e}_i\}$) restricts the wavevectors such that $\mathbf{k}\cdot\mathbf{e}_i = 2\pi n$ for all i, where $n \in \mathbb{Z}$. Since the zero wavevector is removed from the spectrum in the expressions above, one must define

$$\hat{\chi}(\mathbf{0}) \equiv \lim_{N,V\to+\infty} \hat{\chi}(\|\mathbf{k}\| = k_{\min}), \tag{26}$$

with a similar expression for $S(\mathbf{0})$. The limit here is taken at constant number density $\rho = N/V$, and $k_{\min}$ is the smallest computable wavevector as determined by the shape of the boundary. To obtain radially-symmetric forms of the structure factor and spectral density, we radially average over all wavevectors with equal magnitude.

Our results for the structure factors and spectral densities of the binary and polydisperse MRJ hard disk packings are shown in Figure 2. The structure factors for these systems lacks Bragg peaks, reflecting the absence of long-range order. Of particular importance is the behavior of the structure factor near the origin. A fit of the small-k region ($k \lesssim 0.5$) with a third-order polynomial suggests $S(0) \approx 0.104 > 0$, meaning that the point pattern generated by the disk centers does not possess vanishing infinite-wavelength local number density fluctuations, an observation verified by direct calculation of the number variance in Figure 3. Note that the local number variance asymptotically scales with the volume of the observation window. This behavior differs from MRJ packings of *monodisperse* spheres in three dimensions [47], where the structure factor decays linearly to zero for small wavenumbers. Bidisperse distributions of disks are inherently *inhomogeneous* with respect to the locations of the particle centers. For the systems studied here, the large concentration of small particles results in local clusters that are essentially close-packed. However, the introduction of large particles into the system generates effective grain boundaries between these local clusters, breaking the uniformity of the underlying point pattern.

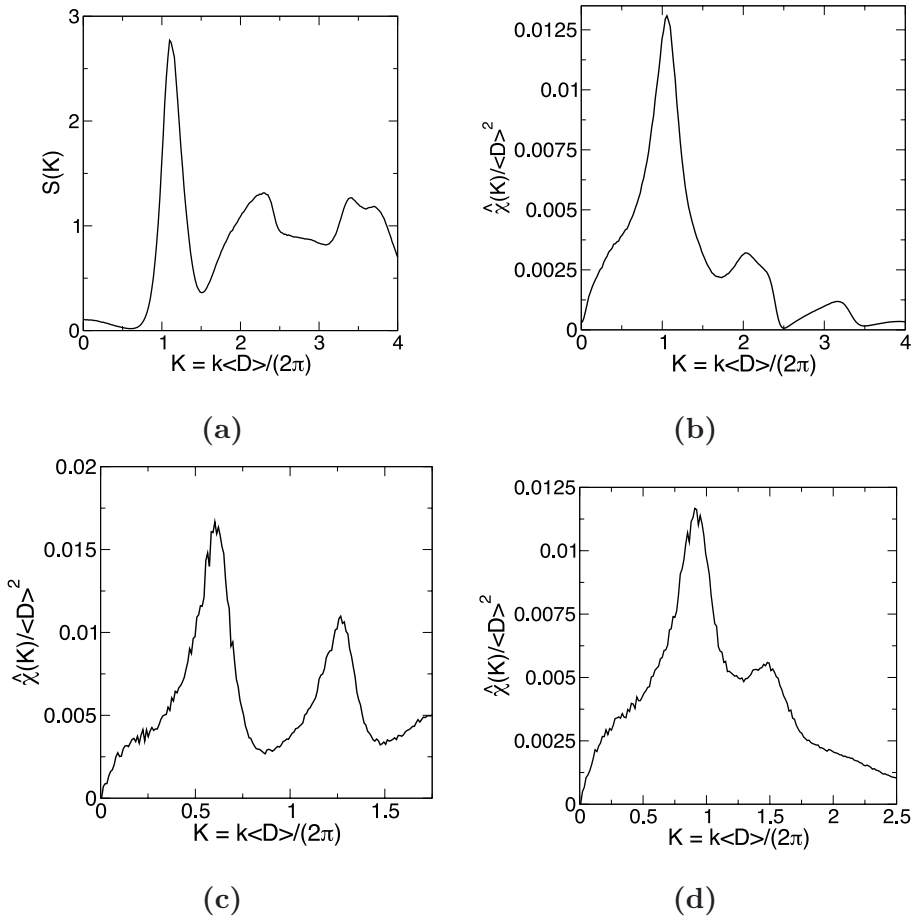

FIG. 2. (a) Structure factor $S(k)$ for a binary packing of disks near the MRJ state. (b) The corresponding spectral density $\hat{\chi}(k)$. Note that infinite-wavelength local density fluctuations are not suppressed unlike local volume fraction fluctuations on the equivalent length scale. (c) Spectral density for particle concentrations $\gamma_{\rm small} = 2/3$ and $\gamma_{\rm large} = 1/3$ with size ratio $\beta = 2.5$. Hyperuniformity of the packing is unaffected by changes in these parameters as expected by the Torquato-Stillinger conjecture. (d) Spectral density for a polydisperse MRJ packing of disks with a uniform distribution of radii in the interval $[R_{\rm min}, R_{\rm max}]$.

We note that the structure factor for our binary packing can be decomposed as

$$S(k) = S_S(k) + S_L(k) + S_C(k), \tag{27}$$

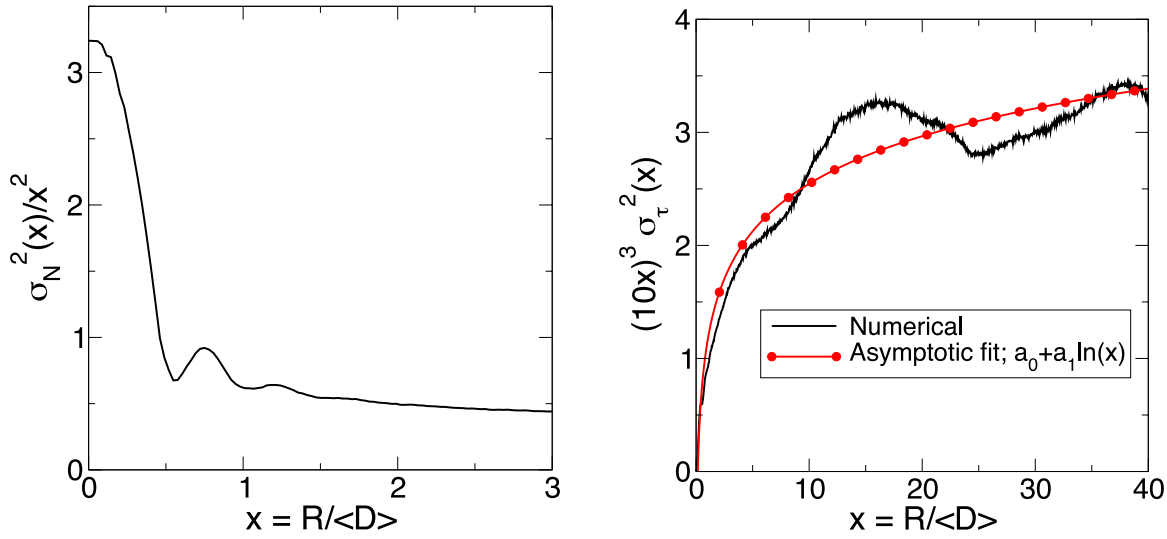

(a) **(b)**

FIG. 3. (Color online) (a) Asymptotic fluctuations in the local number density for the MRJ binary disk packing. (b) Asymptotic fluctuations in the local volume fraction for the binary MRJ packing, demonstrating that the system is indeed hyperuniform.

where

$$S_S(k) = \frac{\left|\sum_{j=1}^{N_S} \exp(-i\mathbf{k}\cdot\mathbf{r}_j)\right|^2}{N} \tag{28}$$

$$S_L(k) = \frac{\left|\sum_{j=1}^{N_L} \exp(-i\mathbf{k}\cdot\mathbf{x}_j)\right|^2}{N} \tag{29}$$

$$S_C(k) = 2\mathrm{Re}\left\{\frac{\left[\sum_{j=1}^{N_S} \exp(-i\mathbf{k}\cdot\mathbf{r}_j)\right]\left[\sum_{\ell=1}^{N_L} \exp(i\mathbf{k}\cdot\mathbf{x}_\ell)\right]}{N}\right\} \tag{30}$$

are the particle structure factors incorporating small-small, large-large, and small-large correlations, respectively. Note that N_S is the number of small particles with positions $\{\mathbf{r}_i\}$, and N_L is the number of large particles with positions $\{\mathbf{x}_i\}$. These partial contributions to the structure factor are shown in Figure 4. None of the partial contributions to the structure factor possess a vanishing small-wavenumber region, implying that the local density fluctuations of the small and large particles each scale with the volume of an observation window as does the covariance. These observations clearly demonstrate that information contained in the structure factor is not sufficient to characterize the packings because it neglects the details of the particle shapes.

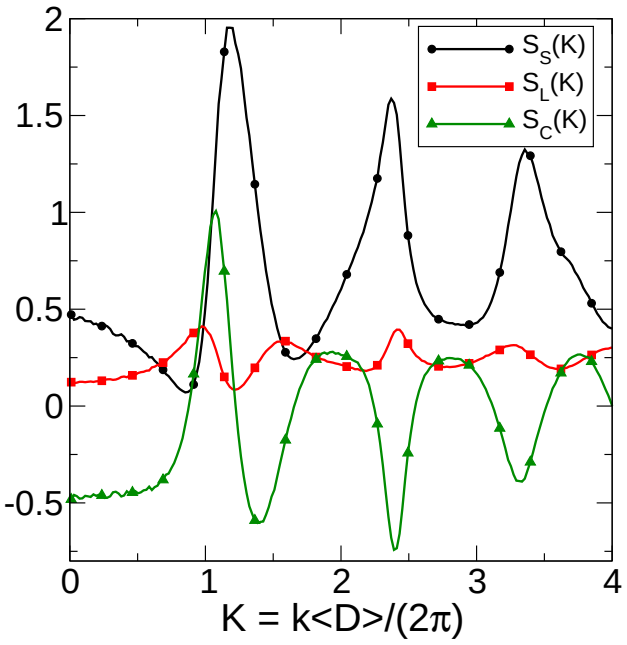

FIG. 4. (Color online) Partial contributions $S_S(k)$, $S_L(k)$, and $S_C(k)$ to the structure factor of the binary MRJ disk packings.

A direct calculation of the spectral density for the binary MRJ system shows markedly different behavior from the structure factor as seen in Figure 2. One notices that infinite-wavelength local-volume-fraction fluctuations are suppressed by the system. We have fit the small-k region of the spectral density (in units of $\langle D\rangle_R^2$) using a third-order polynomial of the form $a_0 + a_1 K + a_2 K^2 + a_3 K^3$ and have found $a_0 = (1.0 \pm 0.2) \times 10^{-5}$, strongly suggesting that this system is hyperuniform with respect to local-volume-fraction fluctuations. We have verified this claim by directly calculating the variance in the local volume fraction, shown in Figure 3. The local-volume-fraction fluctuations decay faster than the volume of an observation window and logarithmically slower than the surface area, consistent with the presence of QLR correlations.

C. Properties of the spectral density of binary MRJ hard disk packings

The spectral density is dominated by a peak with wavelength just below $\langle D\rangle_R$, approximately corresponding to the small-particle diameter. This observation is consistent with the microstructure of the medium, which contains several regions of almost close-packed clusters of small particles. In order to further understand the behavior of the spectral density, it is

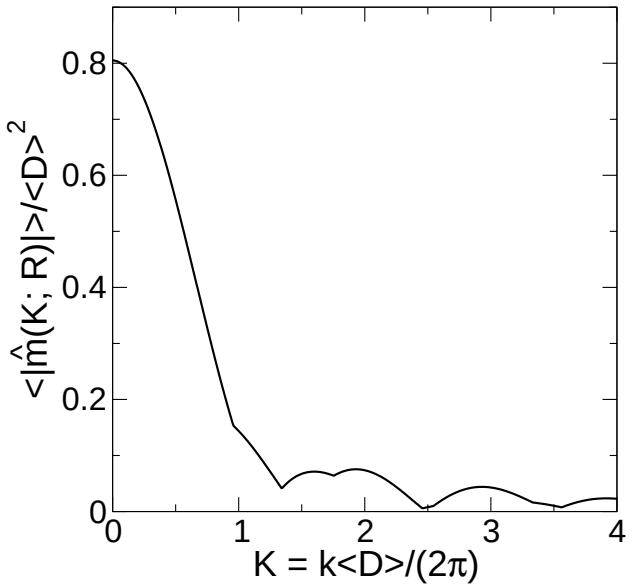

FIG. 5. The average magnitude $\langle|\hat{m}(k;R)|\rangle_R$ of the spatial contribution to the spectral density.

important to recognize that both the local distribution of inclusions and the shape information of the particles contribute to $\hat{\chi}$. However, the relative influence of each component on the spectral density varies throughout the spectrum. To characterize this effect, we recall the representation (24) of the spectral density, which admits the following upper bound:

$$\hat{\chi}(\mathbf{k}) \leq N\rho\left(\langle|\hat{m}(k;R)|\rangle_R\right)^2. \tag{31}$$

Figure 5 plots the average $\langle|\hat{m}(k;R)|\rangle_R$, which according to (31) controls the upper bound on the spectral density. Note that for small wavenumbers $[k\langle D\rangle_R/(2\pi) \lesssim 2]$ the bound (31) places only weak constraints on the spectral density, implying that this region of the spectrum is controlled by information in the local structure of the heterogeneous medium. We emphasize that the shape information of the particles must still be included at small wavenumbers to account for vanishing infinite-wavelength local-volume-fraction fluctuations, but, as we show below, such geometric information only provides the appropriate weights for the partial contributions to the structure factor to induce hyperuniformity. In constrast, the large-wavenumber region of the spectrum closely follows the behavior of the upper bound (31), meaning that the length scale imposed by the decoration of the particle centers, here chosen to be disks, controls the spectral density. We emphasize that this portion of the spectrum arises from the shape information of the inclusions themselves and is almost entirely independent of the distribution of particles in the system. Specifically, the particle indica-

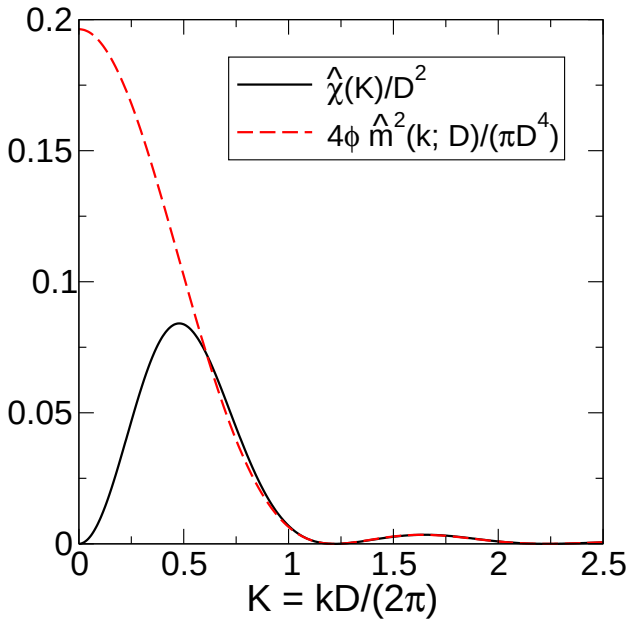

FIG. 6. (Color online) Spectral density and corresponding shape contribution for a microstructure generated by the step-function g_2 process. Note that the shape contribution controls the spectral density for large wavenumbers.

tor function $m(r;R)$, which has compact support $[0,R]$, possesses a Fourier representation $\hat{m}(k;R)$ that is both long-ranged and has an intrinsic period, which for a binary packing leads to interference effects in the large-wavenumber region.

Similar behavior arises in monodisperse systems, where the spectral density is exactly given $\hat{\chi}(k) = \rho\hat{m}^2(k;R)S(k)$, and one can rigorously separate information contained in the point pattern generated by the sphere centers from the shape information of the inclusions. Figure 6 shows the spectral density and shape contribution for a system of impenetrable disks with pair correlation function $g_2(r) = \Theta(D-r)$. Note that the bound (31) only applies when $S(k)$ is at a maximum; for clarity we have omitted the associated scaling factor on the shape contribution. As with the binary MRJ packing, this "step-function process" possesses a spectral density that for small wavenumbers depends signficantly on the distribution of sphere centers; the large-wavenumber region is almost exactly equal to the shape contribution since the structure factor approaches an asymptotic value of unity. Although for binary systems polydispersity precludes the direct separation of the shape information from the underlying point pattern, these examples show that qualitatively these components continue to affect only specific portions of the spectral density.

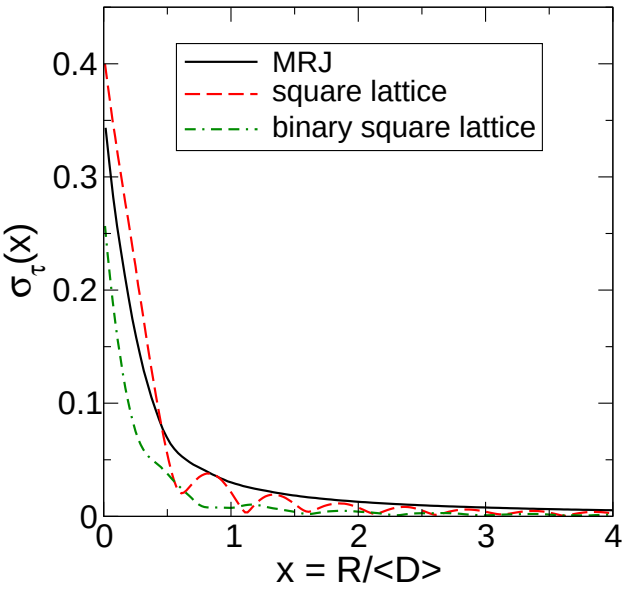

FIG. 7. (Color online) Standard deviation of the local volume fraction for the close-packed binary square and square lattices with the corresponding result for the MRJ binary packing.

The dominance of the shape information for large wavenumbers has the surprising effect of almost completely suppressing fluctuations for $K = k\langle D\rangle_R/(2\pi) \approx 2.5$, thereby suggesting that local volume fraction fluctuations essentially vanish on this length scale. In actuality, the nonuniformity of the microstructure precludes a complete extinction of the variance in the local volume fraction; nevertheless, the local-volume-fraction variance (Figure 7) undergoes a sharp change in slope near this length scale, highlighting a transition to the "geometrically-controlled" region of the spectral density. Physically, this behavior implies that observation windows with radii given by the appropriate wavelength capture the effective pore size surrounding the inclusions in such a way that the medium is essentially homogeneous on this *local* scale. This observation suggests that the void space surrounding the particles plays a central role in determining the spatial statistics of a heterogeneous system.

D. Probing the origin of QLR pair correlations

It is important to note that the small-k behavior of the spectral density for the binary MRJ packing results in an "anomalous" asymptotic scaling of the variance in the local volume fraction. Specifically, our results suggest that the spectral density is nonanalytic at the origin with an expansion $\hat{\chi}(k) \sim a_1 k + \mathcal{O}(k^2)$ as $k \to 0$, implying that the autocovariance

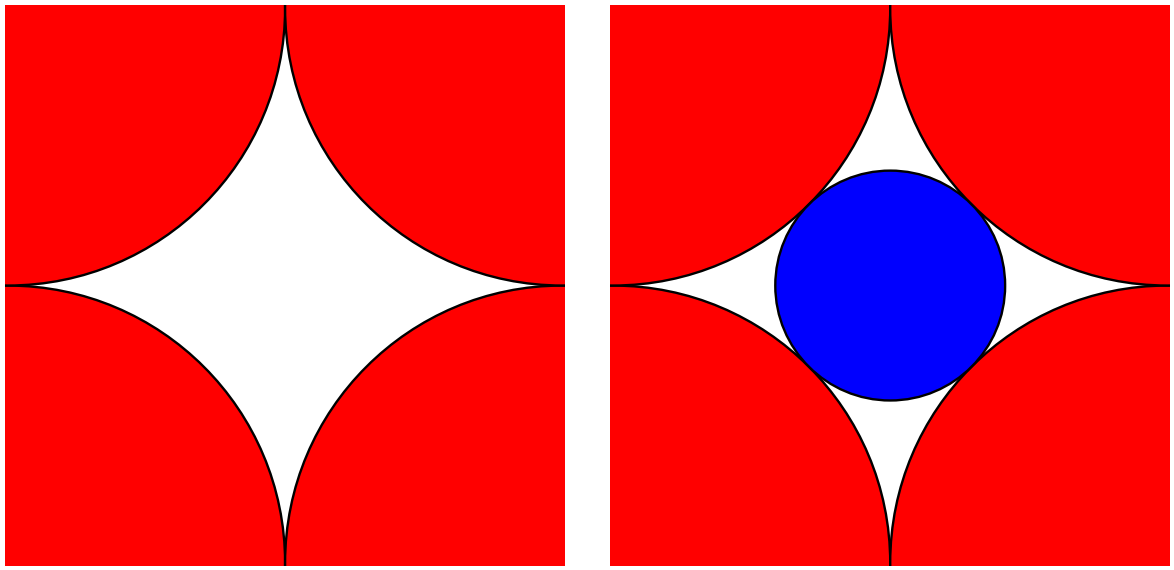

(a) **(b)**

FIG. 8. (Color online) (a) Unit cell for the square lattice at close-packing. (b) Unit cell for a close-packed binary variant of the square lattice.

function exhibits quasi-long-range behavior and scales with r^{-3} [$r^{-(d+1)}$ in d dimensions]. Equivalent behavior has been observed for the structure factor of MRJ monodisperse sphere packings in three dimensions [4], and the number variance in that case has been shown to scale according to:

$$\sigma_N^2(R) \sim (b_0 + b_1 \ln R)R^2 + \mathcal{O}(R). \tag{32}$$

A related scaling must also hold for the variance in the local volume fraction of our binary MRJ packings; specifically:

$$\sigma_\tau^2(R) \sim \frac{(c_0 + c_1 \ln R)}{R^3} + \mathcal{O}(R^{-4}). \tag{33}$$

One can directly see the effect of this behavior in Figure 7, where the variance in the local volume fraction for the MRJ packings is compared to the square lattice packing and its binary variant, the unit cells for which are shown in Figure 8. Note that local volume fraction fluctuations in the MRJ packings decay more slowly than in either of the periodic systems; indeed, as the size distribution of the void space becomes smaller and more uniform, local-volume-fraction fluctuations are more rapidly suppressed on the global scale of the microstructure. Since the integer packing is not even strictly jammed, this comparison suggests

that strict jamming is neither a necessary nor a strong determinant of hyperuniformity in heterogeneous media.

Identifying the origin of the linear small-wavenumber region of the spectral density is an open problem that must be related to the structural features of the MRJ state. This problem is particularly difficult for our polydisperse packings since the underlying point pattern generated by the particle centroids possesses non-vanishing infinite-wavelength local number density fluctuations. However, the spectral density $\hat{\chi}(k)$ can be expressed in terms of the partial structure factors as

$$\hat{\chi}(k) = \rho\hat{m}^2(k;R_S)S_S(k) + \rho\hat{m}^2(k;R_L)S_L(k) + \rho\hat{m}(k;R_S)\hat{m}(k;R_L)S_C(k), \tag{34}$$

where R_S and R_L are the radii of the small and large particles, respectively. This result follows directly from an expansion of (24). As $k \to 0$, we therefore find

$$\hat{\chi}(0) = \rho v^2(R_S)S_S(0) + \rho v^2(R_L)S_L(0) + \rho v(R_S)v(R_L)S_C(0), \tag{35}$$

implying that the particle volumes provide the appropriate *weights* to properly balance the small- and large-particle variances with the covariance between the particles. Additionally, since $\hat{m}(k;R)$ possesses no linear term in its small-wavenumber Taylor expansion, it follows that the appearance a linear small-wavenumber region in the spectral density, and therefore QLR correlations, *must* involve an appropriate superposition of linear contributions in the partial structure factors.

This observation suggests that quasi-long-range correlations in MRJ packings arise from the competing effects of strict jamming and maximal randomness. Incompressibility of the structure from strict jamming implies that particles should be correlated over several characteristic length scales; indeed, along the equilibrium branch of the binary hard-disk phase diagram, one expects that correlations become fully long-ranged at the close-packed density, corresponding to phase-separated lattice structures [54]. However, maximal randomness interferes with this long-range order, resulting in the apparent $r^{-(d+1)}$ asymptotic scaling in the pair correlation function. For our binary packings, this scaling is encoded in the partial pair correlations of the structure, which, after appropriate weighting with the shape information of the particles, induces hyperuniformity.

We emphasize that a complete explanation for the appearance of the linear small-wavenumber region of the spectral density is intractable because the problem is inherently

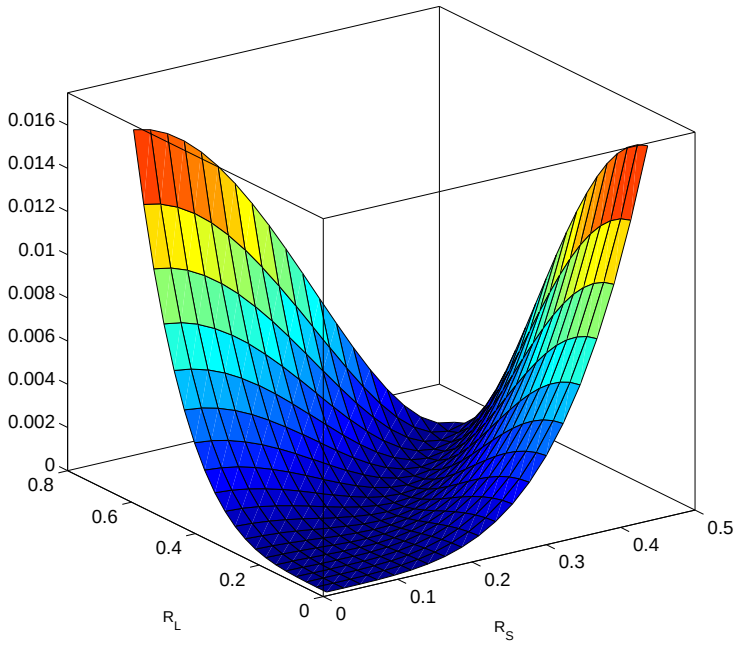

FIG. 9. (Color online) The quadratic form (35), equal to the small-wavenumber limit of the spectral density $\hat{\chi}(0)$, as a function of the radii of the particles in the packing. A uniform decrease in the particle radii defines a basin of hyperuniform systems.

non-local due to hyperuniformity and the presence of QLR correlations. Furthermore, it has recently been established that decreasing the exponential scaling of the small-wavenumber is associated with greater disorder within a many-particle system, potentially even inducing clustering among the particles [55], an effect clearly inconsistent with strict jamming. More generally, hyperuniformity is associated with an effective interparticle repulsion that attempts to evenly distribute the particles throughout space, and the length scale of this repulsion increases with increasing exponential scaling of the small-wavenumber region of the spectral density [55]. The conditions of saturation and impenetrability in an MRJ packing induce structural order that apparently competes with the constraint of maximal randomness to minimize the scaling of the small-wavenumber region of the spectral density to its smallest integer value, an effect that we argue is physically tied to the void-space distribution of the system.

To motivate our discussion of the void space and its fundamental importance to polydisperse MRJ packings, we mention a peculiar property of hyperuniformity in these packings.

Namely, one can maintain hyperuniformity in polydisperse MRJ hard-particle systems even upon shrinking the particles at a fixed size ratio so long as one does not affect the underlying statistical distribution of the point process; this effect is illustrated in Figure 10. To understand this behavior, we note that the leading-order term governing the expansion of the Fourier transform of the particle indicator function $\hat{m}(k;R)$ is the volume of the particle πR^2, meaning that for small wavenumbers we have (in the case of the binary packings)

$$\hat{\chi}(\mathbf{k}) \sim \frac{1}{V}\left|\pi R_{\text{small}}^2 \sum_{j=1}^{N_{\text{small}}} \exp(i\mathbf{k}\cdot\mathbf{r}_j) + \pi R_{\text{large}}^2 \sum_{\ell=1}^{N_{\text{large}}} \exp(i\mathbf{k}\cdot\mathbf{r}_\ell)\right|^2, \tag{36}$$

which, upon rescaling $R_i \to \kappa R_i$ for $\kappa < 1$, suggests

$$\hat{\chi}_{\text{shrink}}(\mathbf{k}) \sim \kappa^4 \hat{\chi}_{\text{MRJ}}(\mathbf{k}) \qquad (k \to 0). \tag{37}$$

Therefore, hyperuniformity of the MRJ binary packing is not lost when performing this scaling operation. Physically, the small-wavenumber region of the spectral density effectively homogenizes the medium due to the coupling between the wavenumber and the particle radius in the indicator function $\hat{m}(k;R)$, meaning that this region is not affected by changes at the boundaries of the particles so long as the underlying statistics of the point pattern generating the medium remain constant. This observation suggests that a saturated and strictly jammed sphere packing extends naturally to an uncountably infinite family of hyperuniform heterogeneous media related by an appropriate scaling parameter. One can map this behavior directly using the result (35), which indicates that the spectral density at small wavenumbers defines a quadratic form in the particle radii when the underlying point pattern of the disk centers is held fixed; the corresponding curve is plotted in Figure 9. Furthermore, this scaling has the effect of deforming the void space surrounding the particles in a *uniform* manner that preserves the regularity of the pore distribution even upon breaking both the jamming and saturation constraints. The medium therefore is able to retain information from the strictly jammed configuration even upon relaxing the sizes of the inclusions. Additionally, it follows from the quadratic form (35) that *non-uniform* changes in the particle radii inherently break the hyperuniformity of the packing.

This behavior has important implications for MRJ packings. First, this effect is geometric in origin and depends on the explicit inclusion of particle shape information to appropriately balance the partial structure factors of the packing. This observation immediately

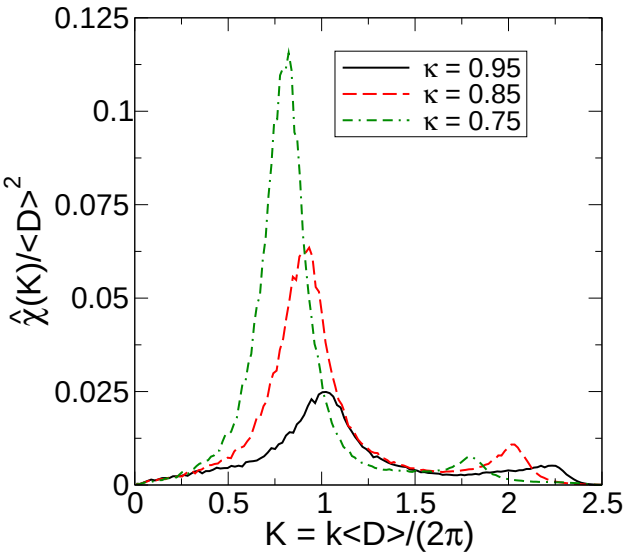

FIG. 10. (Color online) Spectral densities upon shrinking the particles in the binary MRJ packings at fixed size ratio $\beta = R_{\text{large}}/R_{\text{small}}$. The parameter $\kappa = R_{\text{shrink}}/R_{\text{MRJ}}$ is the scaling factor.

implies that "point" information contained in the particle centers is not sufficient to describe the system. Second, the presence of interparticle contacts is not essential for the onset of hyperuniformity and QLR correlations. This subtle point, though easy to appreciate mathematically, is highly nontrivial from a physical perspective. It implies that on the *global* scale of the microstructure, the space is regularized in such a way that hyperuniformity is preserved upon making uniform scaling deformations of the particle phase. Importantly, since the spectral density is a descriptor of both the particle and the void phases, this homogenization is invariant to the choice of reference phase. Note in particular that upon breaking the contact network of the MRJ packing, the void space can become *connected* throughout the space, implying that the spatial statistics of the microstructure must account for correlations over large length scales. It is for these reasons that we turn our attention to the void-space distribution in the following sections.

Note that our scaling analysis does not apply if the particle radii are uniformly increased since breaking the impenetrability constraint implies that higher-order microstructural information is necessary to characterize the medium, and (36) is no longer valid. Additionally, if the particles are shrunk to the point that the small particle radius vanishes, then the packing will no longer be hyperuniform since important shape information about the system has been lost. In terms of the void space, the distribution of pore sizes will be skewed

toward higher values due to the sudden appearance of "holes" in the microstructure, corresponding to the lost small particles, thereby de-regularizing the microstructure and breaking hyperuniformity.

IV. CHARACTERIZATION OF THE PORE-SIZE DISTRIBUTION

A. Numerical evaluation of pore-size statistics

It is clear from the discussion above that the void phase surrounding the disk inclusions of the binary MRJ packings plays a significant role in characterizing local fluctuations in the medium. Indeed, we argue that the conditions of strict jamming and saturation place strong constraints on the distribution of the pore sizes, effectively regularizing the local structure around each disk such that the system is hyperuniform with respect to local-volume-fraction fluctuations even though the disk centers do not consitute a hyperuniform point pattern. To support our arguments concerning the void space, we have quantified the size of the available void space using the so-called *complementary pore-size cumulative distribution function* $F(\delta)$ [11], which represents the fraction of the void space external to the inclusion phase with a pore radius larger than δ. Equivalently, if we define $P(\delta)$ as the probability density that a randomly chosen point in the void space lies within δ and $\delta + d\delta$ from the *nearest* point on the void-inclusion interface, then:

$$F(\delta) = \int_{\delta}^{+\infty} P(\Delta) d\Delta. \tag{38}$$

Figure 11 shows the cumulative pore-size distribution function for the binary MRJ packings along with the corresponding results for the integer and binary integer packings and a system of equilibrium monodisperse hard disks at volume fraction $\phi = 0.5$. The equilibrium hard disk packing is neither saturated nor jammed; it is also known that this system is not hyperuniform [5]. As a result, it possesses a broad distribution of pore sizes, and the probability of finding large pores (i.e., on the order of a particle diameter) is nonvanishing. In contrast, both the integer packing and its binary variant possess narrow pore-size distributions with compact supports, which result from the close-packed nature of the packings. Interestingly, Figure 11 indicates that the binary MRJ packing also possesses a narrow pore-size distribution that essentially falls between the square and binary square packings.

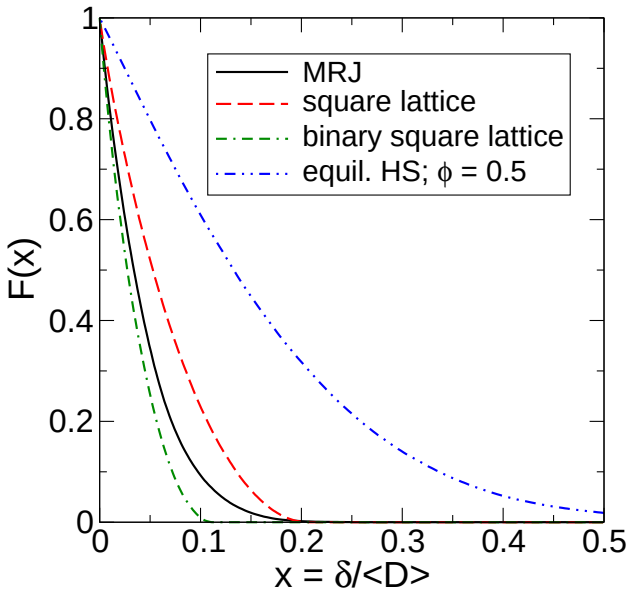

FIG. 11. (Color online) Cumulative pore-size distributions F for the binary MRJ packing, the square lattice $\mathbb{Z}^2$, a saturated binary variant of $\mathbb{Z}^2$, and a system of equilibrium hard spheres with volume fraction $\phi = 0.5$.

This observation suggests that the void space is highly constrained by the condition of strict jamming and almost regular in its distribution.

One can directly compute the moments $\langle \delta^n \rangle$ of the pore size density from the cumulative distribution $F(\delta)$ using the relation [11]:

$$\langle \delta^n \rangle = n \int_0^{+\infty} \delta^{n-1} F(\delta) d\delta. \tag{39}$$

Lower-order moments of the pore-size density arise in bounds on the mean survival times and principal relaxation times of heterogeneous materials and are thus important descriptors of microstructures [56, 57] (see Section V.B below). Table I provides the first moments and standard deviations of the pore size for the systems mentioned in Figure 11. The average pore sizes for the hyperuniform systems are significantly smaller than for the equilibrium hard disk packing. In fact, the pore size distribution of the binary MRJ packing appears to be more localized about its mean than even the integer packing. We conclude from this information that the available void space in the binary MRJ disk packing is sufficiently restricted such that local volume fraction fluctuations decay faster than the volume of an observation window, thereby reflecting the underlying regularity of the pore space.

TABLE I. First moments and standard deviations of the pore size for distributions of hard disks.

	$\langle\delta\rangle/\langle D\rangle$	$\sigma_\delta/\langle D\rangle$
binary MRJ	0.0438	0.0380
$\mathbb{Z}^2$	0.0626	0.0480
binary $\mathbb{Z}^2$	0.0332	0.0258
equil. HS ($\phi = 0.5$)	0.1612	0.1267

B. Bounds on the pore size distribution

It is important to note that the pore-size distribution for a hyperuniform hard-particle packing with volume fraction ϕ must asymptotically decay faster than the corresponding distribution for a non-hyperuniform medium with the same one-point statistics; this claim is a generalization of an argument by Gabrielli and Torquato [15]. Since non-hyperuniform media are by definition "Poisson-like," it suffices then to consider the pore-size distribution for a polydisperse system of fully penetrable disks. The cumulative pore-size distribution $F_P(\delta)$ for such a system is known analytically [11, 33] and is given by

$$F_P(\delta) = (1/\phi_1)\exp\left[-\rho\langle v(\delta + R)\rangle_R\right], \tag{40}$$

where the angular brackets denote an average over the disk radii and ϕ_1 is the volume fraction of the matrix phase. We emphasize in these calculations that we are considering the pore-size distribution for a 2D *Poisson-distributed* heterogeneous medium with volume fraction ϕ that is the *same as a reference hyperuniform system*. However, equivalence of the one-point statistics does not imply that the number densities are the same between the systems. To account for this discrepancy, we write $\rho = \eta/(\pi\langle R^2\rangle_R) = \ln(1/\phi_1)/(\pi\langle R^2\rangle_R)$, which implies

$$F_P(\delta) = \exp\left[-(s\langle D\rangle_R/\phi_1)\tilde{\delta}^2 - (s\langle D\rangle_R/\phi_1)\tilde{\delta}\right], \tag{41}$$

where $s = \rho\phi_1\langle s(R)\rangle_R$ is the specific surface of a Poisson-distributed medium and $s(R)$ is the surface area of a d-dimensional sphere of radius R. Note that we have introduced the length scale $\langle D\rangle_R$ and reduced variable $\tilde{\delta} = \delta/\langle D\rangle_R$ in (41). Letting $b = s\langle D\rangle_R/\phi_1$, we find

the following upper bounds for the first and second moments of the pore size density:

$$\langle\tilde{\delta}\rangle_{\mathrm{UL}} = \frac{1}{2}\sqrt{\frac{\pi}{b}}\exp\left[b/4\right]\mathrm{erfc}\left(\sqrt{b}/2\right) \tag{42}$$

$$\langle\tilde{\delta}^2\rangle_{\mathrm{UL}} = \frac{1}{b}\left(1 - b\langle\tilde{\delta}\rangle_{\mathrm{UL}}\right). \tag{43}$$

The above Poisson bound will be rigorously true for the full pore-size distribution of our polydisperse MRJ packings based solely on the presence of hyperuniformity. However, we can significantly tighten the bounds of the moments of the pore-size distribution for binary MRJ packings based on our analysis below of the local voids. Specifically, since the distribution of voids within the MRJ packings is dominated by three- and four-particle loops, the average pore size must be less than the corresponding average pore size of a saturated integer lattice. This effect is explicitly shown in Figure 11, where it is clear that the integer lattice provides a good approximate upper bound for the full pore-size distribution with the exception of the tail, due to the presence of higher-order loops in the MRJ packing. Since this tail must decrease faster than exponentially with a cut-off at the small-particle radius (because of saturation), we therefore have the following tighter upper bounds on the first and second moments of the pore size distribution:

$$\langle\tilde{\delta}\rangle \leq \langle\tilde{\delta}\rangle_{\mathbb{Z}^2} \tag{44}$$

$$\langle\tilde{\delta}^2\rangle \leq \langle\tilde{\delta}^2\rangle_{\mathbb{Z}^2}. \tag{45}$$

It is also possible to find a simple lower bound on the pore-size distribution that is applicable for arbitrary heterogeneous media (hyperuniform or not). Specifically, we utilize the following series representation for the cumulative pore-size distribution [11]:

$$F(\delta) = \frac{1}{\phi_1}\left[1 + \sum_{k=1}^{+\infty}(-\rho)^k\left(\frac{1}{\Gamma[k+1]}\right)\int\left\langle g_k(\mathbf{r}^k; R^k)\prod_{j=1}^{k} m(\|\mathbf{x}-\mathbf{r}_j\|; \delta + R_j)\right\rangle_{R^k} d\mathbf{r}_j\right]. \tag{46}$$

It is well-known that keeping terms up to order ρ^k in (46) places an upper bound on $F(\delta)$ for k even and enforces a lower bound for k odd [11]. Therefore, by expanding the series to order ρ we obtain the following lower bound on $F(\delta)$:

$$F(\delta) \geq \max\left\{\frac{1}{\phi_1}\left[1 - \rho\langle v(\delta + R)\rangle_R\right], 0\right\}; \tag{47}$$

the max operation in (47) enforces the trivial lower bound $F(\delta) \geq 0$. Note that (47) is equivalent to the $\mathcal{O}(\rho)$ expansion of the pore-size distribution for a Poisson-distributed

medium; however, the number density (and therefore the specific surface) of the system is not necessarily the same as the Poisson medium. We will now assume that our hyperuniform reference medium consists of impenetrable spheres with volume fraction $\phi = \rho\langle v(R)\rangle_R$; we also remark that the definition of the specific surface for impenetrable spheres $s = \rho\langle s(R)\rangle_R$ is different than for a fully-penetrable system. It now follows that

$$F(\delta) \geq \max\left\{1 - b\tilde{\delta}^2 - b\tilde{\delta}, 0\right\}, \tag{48}$$

where $b = s\langle D\rangle_R/\phi_1$ as in the Poisson case. The lower bound (48) first reaches zero at

$$\tilde{\delta^*} = \frac{-1 + \sqrt{1 + 4/b}}{2}. \tag{49}$$

We thus obtain the following lower bounds on the first and second moments of the pore size density

$$\langle\tilde{\delta}\rangle_{\mathrm{LL}} = \tilde{\delta^*} - \frac{b\tilde{\delta^*}^2}{2} - \frac{b\tilde{\delta^*}^3}{3} \tag{50}$$

$$\langle\tilde{\delta}^2\rangle_{\mathrm{LL}} = \tilde{\delta^*}^2 - \frac{2b\tilde{\delta^*}^3}{3} - \frac{b\tilde{\delta^*}^4}{2}. \tag{51}$$

Figure 12 plots the upper and lower bounds (42) and (50) on the mean pore size for hyperuniform binary heterogeneous media at volume fraction ϕ. We emphasize that these bounds account only for the hyperuniformity of the packings and thus place constraints on the pore-size distributions of *any* binary hyperuniform hard-particle packing.

For our binary MRJ packings, the specific surface is

$$s_{\mathrm{MRJ}}\langle D\rangle_R/\phi_1 = (\phi/\phi_1)\langle D\rangle_R^2/\langle R^2\rangle_R = (4\phi/\phi_1)\left[\frac{(\gamma_{\mathrm{small}} + \gamma_{\mathrm{large}}\beta)^2}{\gamma_{\mathrm{small}} + \gamma_{\mathrm{large}}\beta^2}\right] \approx 21.6917. \tag{52}$$

The specific surface for the equivalent Poisson-distributed medium is

$$s_P\langle D\rangle_R/\phi_1 = -\ln(\phi_1)\langle D\rangle_R^2/\langle R^2\rangle_R \approx 7.34037; \tag{53}$$

as expected, this value is less than the corresponding result for the impenetrable case. Using these parameters, we collect in Table II the bounds on the pore size of our binary MRJ disk packings. We immediately notice that the numerical values are well within the bounds above; it follows that the one-point statistics of the medium do not place strong constraints on the distribution of the void space. Furthermore, this evidence suggests hyperuniformity strongly regularizes the pore space compared to the Poisson-distributed system.

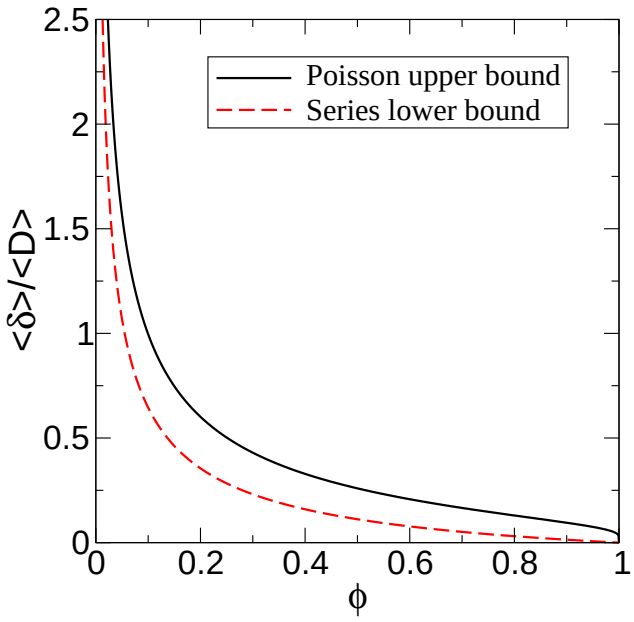

FIG. 12. (Color online) Upper and lower bounds on the mean pore size applicable for binary hyperuniform heterogeneous media at volume fraction ϕ with the same composition as the MRJ binary disk packings studied here.

TABLE II. Bounds on the moments of the pore-size distribution for binary MRJ packings of hard disks.

	$\langle\tilde{\delta}\rangle$	$\langle\tilde{\delta}^2\rangle$
Poisson upper bound	0.1135	0.0227
$\mathbb{Z}^2$ upper bound	0.0626	6.219×10^{-3}
Series lower bound	0.0224	6.635×10^{-4}
MRJ binary packing	0.0438	3.362×10^{-3}

It is interesting to note that the series lower bound provides a better estimate of the mean pore size than the Poisson upper bound. This observation is reasonable since the compact support of the lower bound more closely matches the behavior of the actual pore-size distribution, which also has compact support due to the saturation of the packing. However, it is unclear if the constraint of saturation can be relaxed while still maintaining hyperuniformity in the medium. One can conjecture that so long as the probability of finding a large pore decays faster than the corresponding behavior for a Poisson pattern, then hyperuniformity holds.

Although our results provide a quantitative basis for understanding the appearance of hyperuniformity in polydisperse MRJ packings, a complete explanation for the linear scaling of the small-wavenumber region of the spectral density is still not apparent. Again, we emphasize that this problem is inherently non-local, and its solution must account for the presence of QLR correlations within the packing. Such correlations are difficult to discern with the distribution $F(\delta)$ that we have presented here, which is essentially a one-point descriptor of heterogeneous media [11].

In the following section, we characterize the allowable n-particle loops within a binary MRJ packing. This analysis suggests that the variance in pore sizes is bounded by the strict jamming of the packings, supporting our argument these constraints are sufficient to induce hyperuniformity.

V. CHARACTERIZATION OF n-PARTICLE LOOPS IN MRJ BINARY DISK PACKINGS

The preceding discussion shows how the void space is a *fundamental* descriptor of a two-phase random heterogeneous medium. As we have seen, fluctuations in the local volume fraction contain information about the void space and therefore provide a more complete picture of hyperuniformity in heterogeneous media. Here we quantitatively characterize the voids in MRJ binary disk packings and argue that strict jamming restricts the variance of pore sizes.

An *n-particle void* is associated with a loop of n contacting disks (an *n-particle loop*) in which each disk only contacts two neighbors. These loops are defined topologically, meaning that their identification is invariant to local shears of the particle contacts. The smallest loops contain three mutually contacting particles. The constraint of saturation places an upper bound on the number of particles in a loop, and the largest loop we find in the MRJ binary disk packings contains 6 particles. The number of n-particle loops in a packing decreases rapidly as n increases.

The area of the void associated with a loop can be rigorously computed by substracting the area of particles falling into the polygon constructed by connecting the centers of the disks in the loop. We note that, except for the 3-particle loop, the polygons associated with other n-loops ($n \geq 4$) can be continuously deformed while maintaining the contacts

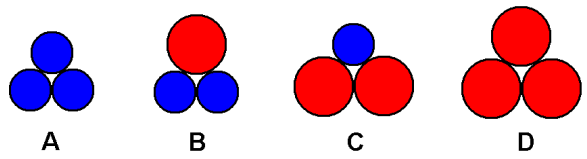

FIG. 13. (Color online) The four distinct 3-particle loops in a binary circular disk packing.

between the particles. Such deformations change the area of the voids associated with the loop. The rigidity of MRJ packings also strongly constrains the number of particles in a loop. In the MRJ packings of binary disks, the majority of the voids involve 3-particle loops, which form the "backbone" of the network. Certain 4-particle loops can be observed at the effective grain boundaries between disks with different sizes. A large portion of these 4-particle loops are very distorted with a void area almost equal to that associated with two 3-particle loops. Loops with more particles are rare in the packings, and the observed ones are all strongly distorted with void areas almost equal to those associated with 3- or 4-particle loops. Therefore, we only discuss the voids associated with 3- and 4-particle loops here, focusing on the maximum possible void areas associated with these loops.

There are four distinct 3-particle loops in the binary disk packings as shown in Figure 13. Defining the radii of small and large disks be R_1 and R_2, respectively, the n-particle void areas $\lambda_{n\alpha}$, normalized by the volume of a small particle, are $\lambda_{3A} \approx 0.0513$, $\lambda_{3B} \approx 0.0631$, $\lambda_{3C} \approx 0.0790$ and $\lambda_{3D} \approx 0.1060$ for a size ratio $\beta = R_2/R_1 = 1.4$. It can be seen clearly that the void areas constitute a small fraction of the small particle area. Since these 3-particle voids dominate the packing, it is reasonable to conclude that the regularity of these local clusters enforces hyperuniformity on the medium despite the nonuniform distribution of the sphere centers.

There are total of six distinct types of 4-particle loops (see Figure 14) in the binary disk packings, each associated with a void that can possess a spectrum of shapes and sizes by distorting the quadrangle formed by the centers of the disks. Although most of the void areas associated with these highly distorted 4-particle loops are almost equal to the area associated with two 3-particle loops, there are still relatively large voids. The maximum normalized void areas are given by $\lambda_{4A} \approx 0.2732$, $\lambda_{4B} \approx 0.3208$, $\lambda_{4C} \approx 0.3934$, $\lambda_{4D} \approx 0.3782$, $\lambda_{4E} \approx 0.4498$ and $\lambda_{4F} \approx 0.5355$. These values are relatively large but more tightly distributed around the mean when compared to the normalized areas for 3-particle voids. As a result, they can be

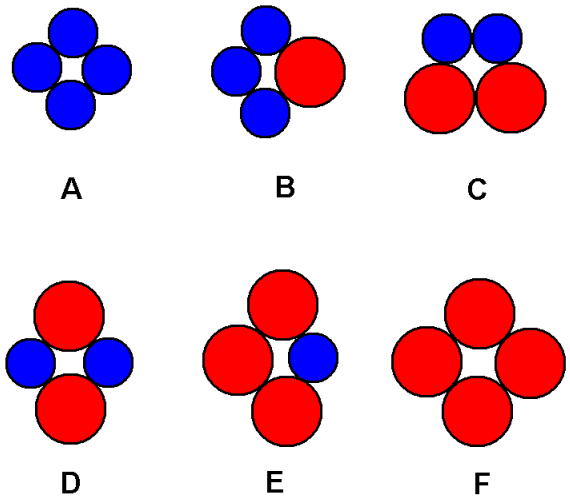

FIG. 14. (Color online) The six distinct families of 4-particle loops in a binary circular disk packing.

considered as an estimate of the upper bound on the degree of local inhomogeneity that can be consistent with hyperuniformity of the packings.

VI. CONCLUDING REMARKS

We have provided a detailed study of local-volume-fraction fluctuations in MRJ packings of polydisperse hard disks and have shown that these systems are hyperuniform with quasi-long-range correlations. Our results strongly suggest that these QLR correlations are a signature of MRJ hard-particle packings, in contrast to previous misconceptions in the literature [24]. Although it is true that the structure factors for these systems do not vanish at small wavenumbers except in the monodisperse limit, we have shown that the more appropriate structural descriptor of MRJ packings is the spectral density, which accounts appropriately for the shape information of the particles. Our work therefore generalizes the Torquato-Stillinger conjecture for hyperuniform point patterns by suggesting that all saturated, strictly-jammed sphere packings are hyperuniform with respect to local-volume-fraction fluctuations. Furthermore, MRJ sphere packings are expected to exhibit quasi-long-range pair correlations scaling as $r^{-(d+1)}$ in d Euclidean dimensions. Importantly, this generalization contains previously-published results for monodisperse MRJ packings [4] as the special case where the particle shape information can be rigorously separated from the

"point" information of the particle centers.

Based on the observations that local-volume-fraction fluctuations are invariant to the choice of reference phase and that one can maintain hyperuniformity in MRJ polydisperse packings under a uniform scaling deformation of the particles, we have argued that the onset of hyperuniformity and quasi-long-range correlations results from the homogenization of the void space external to the particles. The conditions of saturation and strict jamming limit the sizes and shapes of the local voids, which are completely determined by the contact network of particles. Using a local analysis of the voids and rigorous bounds on the pore-size distribution, we have argued that the void space is highly constrained by strict jamming, thereby suppressing infinite-wavelength local-volume-fraction fluctuations. Furthermore, we suggest that the presence of quasi-long-range correlations reflects the inherent structural correlations from the contact network between void shapes. Specifically, saturation and strict jamming of the packings compete with the maximal randomness of the particle distributions to drive the small-wavenumber region of the spectral density to its smallest integer value.

Although our work has addressed important problems related to the structural properties of MRJ hard-particle packings, a number of unanswered questions remain. First, a rigorous foundation for the observed linear scaling in the small-wavenumber region of the spectral density is still missing. This problem is immensely difficult to handle theoretically because the problem is inherently long-ranged, and any local analysis of the MRJ structure will therefore be unable to account correctly for this behavior [26]. Second, although we have considered only polydisperse MRJ packings of d-dimensional spheres, our results are expected to hold more generally for strictly jammed packings of hard particles of arbitrary geometry. Indeed, our arguments concerning the void space of an MRJ packing are easily extended to include these more general cases, and in a companion paper we will provide direct evidence that MRJ packings of hard ellipses and superdisks [58] are also hyperuniform with signature quasi-long-range correlations indicated by linear scaling of the small-wavenumber region of the spectral density. These results will suggest a remarkably strong extension of the Torquato-Stillinger conjecture, namely that all maximally random strictly jammed saturated packings of hard particles, including those with size- and shape-distributions, are hyperuniform with universal quasi-long-range correlations [via the two-point probability function $S_2(r)$] scaling asymptotically as $r^{-(d+1)}$.

We mention that recent, independent work, appearing in preprint form shortly after our

own manuscript was posted, [59] has shown that hyperuniformity and vanishing infinite-wavelength local-volume-fraction fluctuations in saturated MRJ packings of polydisperse disks are consistent with certain fluctuation-response relations involving a generalized "compressibility." However, this work does not address the appearance of quasi-long-range pair correlations in MRJ hard-particle packings and does not consider MRJ packings of non-spherical particles as in our companion paper [58].

Our arguments suggest in particular that certain quantum many-body systems and cosmological structures with the same linear small-wavenumber scaling in the structure factor [7, 9, 10] are statistically "rigid" in the sense that their microstructures are effectively homogeneous over large length scales with vanishing infinite-wavelength number density fluctuations. These unique features are inherently linked to the *structural* properties of the system, independent of the physical model itself.

Finally, we note that the systems examined in this paper are constrained to be both saturated and strictly jammed. Saturation of the packings is responsible for enforcing compact support in the pore-size distribution function and therefore plays an important role in regularizing the void space surrounding the jammed disks. However, it is not clear if saturation is a necessary condition to ensure hyperuniformity in strictly jammed heterogeneous media; this situation corresponds to a weakening of the Torquato-Stillinger conjecture. Namely, what conditions must a strictly jammed but unsaturated packing of hard spheres meet in order to be hyperuniform? We note that the event-driven molecular dynamics algorithm used here to generated the binary MRJ disk packings inherently precludes the presence of arbitrarily large "holes" within the packing. However, it does produce a small concentration ($\sim$2.5%) of "rattler" particles, which are particles that are free to move within some small caged region of the packing. Removal of such particles is known to break hyperuniformity of the medium even though the strict jamming of the surrounding structure remains [4]; therefore, strict jamming alone is not sufficient to induce hyperuniformity if large holes are "common enough" in the statistics of the microstructure. This scenario corresponds to skewing the pore-size distribution and thereby de-regularizing the void space.

It is indeed possible to construct strictly jammed packings of two-dimensional disks with a hole of arbitrarily large size by starting with a ring of particles encompassing a large pore; this ring can be jammed by surrounding it with a close-packed collection of particles that approximates an impenetrable "wall" (see Figure 15). One is then free to construct any

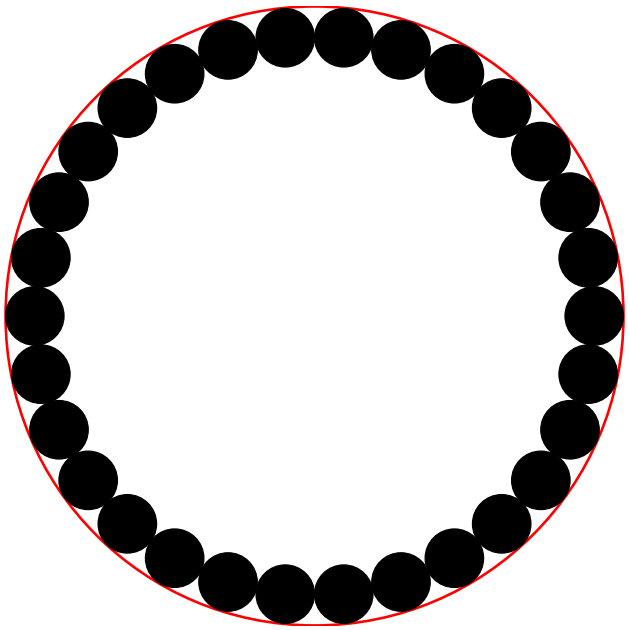

FIG. 15. (Color online) A jammed configuration of particles (up to rotations) surrounding a circular void. By replacing the wall with a close-packed collection of particles, one can construct strictly jammed packings in the plane with pores of arbitrarily large size.

strictly jammed system of particles outside the hole [60]. If such holes are sufficiently rare, then it is possible that the system may still be hyperuniform since the pores do not become very large on average.

ACKNOWLEDGMENTS

This work was supported by the National Science Foundation under Grants DMS-0804431 and DMR-0820341.

---

[1] S. Torquato, T. M. Truskett, and P. G. Debenedetti, Phys. Rev. Lett. **84**, 2064 (2000).

[2] P. M. Chaikin and T. C. Lubensky, *Principles of Condensed Matter Physics* (Cambridge UP, New York, 2000).

[3] J. D. Bernal, Nature (London) **185**, 68 (1960).

[4] A. Donev, F. H. Stillinger, and S. Torquato, Phys. Rev. Lett. **95**, 090604 (2005).

[5] S. Torquato and F. H. Stillinger, Phys. Rev. E **68**, 041113 (2003).

[6] C. E. Zachary and S. Torquato, J. Stat. Mech.: Theory and Expt., P12015 (2009).

[7] S. Torquato, A. Scardicchio, and C. E. Zachary, J. Stat. Mech.: Theory and Expt., P11019 (2008).

[8] A. Scardicchio, C. E. Zachary, and S. Torquato, Phys. Rev. E **79**, 041108 (2009).

[9] L. Reatto and G. V. Chester, Phys. Rev. **155**, 88 (1967).

[10] P. J. E. Peebles, *Principles of Cosmology* (Princeton UP, Princeton, NJ, 1993).

[11] S. Torquato, *Random Heterogeneous Materials: Microstructure and Macroscopic Properties* (Springer, New York, 2002).

[12] A packing in which no space is available to insert an additional particle without violating the impenetrability conditions is called saturated.

[13] The converse statement is not true, meaning that hyperuniformity does not imply strict jamming. The square lattice in two dimensions is one example of a hyperuniform packing that is not strictly jammed.

[14] A. Gabrielli, B. Jancovici, M. Joyce, J. L. Lebowitz, L. Pietronero, and F. S. Labini, Phys. Rev. D **67**, 043506 (2003).

[15] A. Gabrielli and S. Torquato, Phys. Rev. E **70**, 041105 (2004).

[16] A. Gabrielli, M. Joyce, and S. Torquato, Phys. Rev. E **77**, 031125 (2008).

[17] S. Warr and J.-P. Hansen, Europhys. Lett. **36**, 589 (1996).

[18] A. Wax, C. Yang, V. Backman, K. Badizadegan, C. W. Boone, R. R. Dasari, and M. S. Feld, Biophys. J. **82**, 2256 (2002).

[19] S. Torquato and F. Lado, J. Chem. Phys. **94**, 4453 (1991).

[20] B. E. Bayer, J. Opt. Soc. Am. **54**, 1485 (1964).

[21] B. Lu and S. Torquato, J. Opt. Soc. Am. A **7**, 717 (1990).

[22] R. S. Fishman, D. A. Kurtze, and G. P. Bierwagen, J. Appl. Phys. **72**, 3116 (1992).

[23] S. Torquato, Int. J. Solids Structures **37**, 411 (2000).

[24] N. Xu and E. S. C. Ching, Soft Matter **6**, 2944 (2010).

[25] R. Kurita and E. R. Weeks, Phys. Rev. E **82**, 011403 (2010).

[26] S. Torquato and F. H. Stillinger, Rev. Mod. Phys. **82**, 2633 (2010).

[27] C. E. Zachary, Y. Jiao, and S. Torquato, Phys. Rev. Lett., in press (2011); arXiv:1008.2548 (2010).

[28] A *Bravais lattice* is defined by the integer linear combinations of a set of d basis vectors in

$\mathbb{R}^d$. By taking the union of a Bravais lattice with its translate(s) by one or more vectors, one can also form periodic non-Bravais lattices, also known as lattices with a basis in the physics literature. Unless otherwise stated, in this paper we use the term *lattice* to refer exclusively to a Bravais lattice.

[29] Y. Jiao, F. H. Stillinger, and S. Torquato, Phys. Rev. E **81**, 011105 (2010).

[30] B. Lu and S. Torquato, J. Chem. Phys. **93**, 3452 (1990).

[31] S. Torquato and G. Stell, J. Chem. Phys. **77**, 2071 (1982).

[32] S. Torquato and G. Stell, J. Chem. Phys. **78**, 3262 (1983).

[33] D. Stoyan, W. S. Kendall, and J. Mecke, *Stochastic Geometry and its Applications* (Wiley, New York, 1995).

[34] The spectral density possesses the properties of a probability density when normalized by $\chi(\mathbf{0}) = \phi(1-\phi)$; the normalized function $\tilde{g}(\mathbf{k}) = \hat{\chi}(\mathbf{k})/\chi(\mathbf{0})$ is also known as the spectral density.

[35] S. Torquato, J. Chem. Phys. **111**, 8832 (1999).

[36] S. Torquato, Ind. Eng. Chem. Res. **45**, 6923 (2006).

[37] Y. Jiao, F. H. Stillinger, and S. Torquato, Phys. Rev. E **76**, 031110 (2007).

[38] J. A. Quintanilla, Proc. R. Soc. A **464**, 1761 (2008).

[39] S. Torquato and F. H. Stillinger, J. Phys. Chem. B **105**, 11849 (2001).

[40] S. Torquato, A. Donev, and F. H. Stillinger, Int. J. Solids and Str. **40**, 7143 (2003).

[41] S. Torquato and F. H. Stillinger, Expt. Math. **15**, 307 (2006).

[42] Unless otherwise noted, we will use subscripts on the angular brackets to distinguish such radial averages from ensemble averages.

[43] J. A. Given, J. Blawzdziewicz, and G. Stell, J. Chem. Phys. **93**, 8156 (1990).

[44] B. Lu and S. Torquato, Phys. Rev. A **43**, 2078 (1991).

[45] B. D. Lubachevsky and F. H. Stillinger, J. Stat. Phys. **60**, 561 (1990).

[46] B. D. Lubachevsky, F. H. Stillinger, and E. N. Pinson, J. Stat. Phys. **64**, 501 (1991).

[47] A. Donev, S. Torquato, and F. H. Stillinger, Phys. Rev. E **71**, 011105 (2005).

[48] A. Donev, S. Torquato, and F. H. Stillinger, J. Comput. Phys. **202**, 737 (2005).

[49] A. Donev, S. Torquato, and F. H. Stillinger, J. Comput. Phys. **202**, 765 (2005).

[50] Y. Jiao, F. H. Stillinger, and S. Torquato, J. Appl. Phys. **109**, 013508 (2011).

[51] T. M. Truskett, S. Torquato, and P. G. Debenedetti, Phys. Rev. E **62**, 993 (2000).

[52] Although we only consider packings in 2D for this study, our results are expected to apply in higher dimensions as well. We have already seen that our methodology contains known results for 3D monodisperse MRJ sphere packings as a special case, and the arguments we make in this section concerning the constrained void space extend directly to higher-dimensional packings.

[53] One can generalize the expression (24) to include hard particle packings with inclusions of *arbitrary* geometry by appropriate modification of $\hat{m}(\mathbf{k})$.

[54] A. Donev, F. H. Stillinger, and S. Torquato, J. Chem. Phys. **127**, 124509 (2007).

[55] C. E. Zachary and S. Torquato, Phys. Rev. E, in press (2011).

[56] S. Prager, Chem. Eng. Sci. **18**, 227 (1963).

[57] S. Torquato and M. Avellaneda, J. Chem. Phys. **95**, 6477 (1991).

[58] C. E. Zachary, J. Jiao, and S. Torquato, submitted for publication (2011).

[59] L. Berthier, P. Chaudhuri, C. Coulais, O. Dauchot, and P. Sollich, Phys. Rev. Lett. **106**, 120601 (2011); arXiv:1008.2899 (2010).

[60] It is not clear if this analogy can be extended to higher dimensions, where it is intimately related to the problem of finding optimal spherical codes; see: J. H. Conway and N. J. A. Sloane, *Sphere Packings, Lattices and Groups* (Springer, New York, 1999), 3rd ed.